Estuarine nutrient loading affects phytoplankton growth and microzooplankton grazing at two contrasting sites in Hong Kong coastal waters

Bingzhang Chen[1], Hongbin Liu[1,2,*], Michael R. Landry[3], Mianrun Chen[2], Jun Sun[4], Loklun Shek[1], Xihan Chen[1], Paul J. Harrison[1]

[1]Atmospheric, Marine, and Coastal Environment (AMCE) Program, Hong Kong University of Science and Technology, Clear Water Bay, Hong Kong

[2]Department of Biology, Hong Kong University of Science and Technology, Clear Water Bay, Hong Kong

[3]Scripps Institution of Oceanography, University of California at San Diego, La Jolla, California 92093-0227, USA

[4]Key Laboratory of Marine Ecology and Environmental Science, Institute of Oceanology, Chinese Academy of Sciences, Nanhai Road 7th, Qingdao 266071, P. R. China

ABSTRACT: To investigate the effects of enhanced nutrient loading in estuarine waters on phytoplankton growth and microzooplankton grazing, we conducted monthly dilution experiments at 2 stations in Hong Kong coastal waters with contrasting trophic conditions. The western estuarine station (WE) near the Pearl River estuary is strongly influenced by freshwater discharge, while the eastern oceanic station (EO) is mostly affected by the South China Sea. Growth rates of phytoplankton were often limited by nutrients at EO, while nutrient limitation of phytoplankton growth seldom occurred at WE due to the high level of nutrients delivered by the Pearl River, especially in the summer rainy season. Higher chlorophyll *a*, microzooplankton biomass, phytoplankton growth and microzooplankton grazing rates were found at WE than at EO. However, the increase in chlorophyll greatly exceeded the increase in phytoplankton growth rate, reflecting different response relationships to nutrient availability. Strong seasonality was observed at both stations, with temperature being an important factor affecting both phytoplankton growth and microzooplankton grazing rates. Picophytoplankton, especially *Synechococcus*, also exhibited great seasonality at EO, with summer abundances being 2 or 3 orders of magnitude higher than those during winter. Our results confirm that in eutrophic coastal environments, microzooplankton grazing is a dominant loss pathway for phytoplankton, accounting for the utilization of >50% of primary production on average.

KEY WORDS: Phytoplankton · Microzooplankton · Grazing rates · Pearl River estuary · Picoplankton

INTRODUCTION

Coastal eutrophication is a major environmental problem because it can induce harmful algal blooms and hypoxia or anoxia. The Pearl River is the second largest river in terms of discharge in China, and its freshwater discharge has a significant impact on Hong Kong coastal waters, carrying large amounts of nutrients into the South China Sea through the Pearl River estuary (Yin et al. 2000, Yin 2002, Harrison et al. 2008). The dynamics of

phytoplankton blooms have received considerable attention in this region, especially with regard to the nutrient requirements for initiating and sustaining blooms (Yin 2003). To understand the mechanisms controlling phytoplankton biomass under such eutrophication regimes, however, complementary studies on factors affecting phytoplankton loss, including grazing by large and small components of the zooplankton, are also required.

Microzooplankton are dominant consumers of primary production in marine ecosystems and are key

regulators of carbon flux pathways within the food web (Calbet & Landry 2004). One generally accepted paradigm concerning microzooplankton grazing is that the predominance of large phytoplankton cells (typically chain-forming diatoms) in eutrophic waters should lower the fraction of primary production consumed by microzooplankton to less than that in oligotrophic waters (Liu et al. 2002). While no definitive study of this issue has been done using consistent methodologies that address all of the potential loss terms across strong gradients in system trophic status, literature synthesis supports at least a modest decrease (~10 to 15%) in the role of microzooplankton as consumers of phytoplankton from oligotrophic open-ocean waters to coastal and estuarine systems (Calbet & Landry 2004). Large phagotrophic protists, especially dinoflagellates, are nonetheless capable of feeding on larger size classes of phytoplankton, even on cells of their own size (Hansen 1992), and may contribute significantly to loss processes in rich coastal environments (Sherr & Sherr 2007). If so, a substantial portion of the productivity in eutrophic coastal waters may be locked into a tightly coupled cycle of growth-grazing-remineralization processes as in microbially dominated systems of the open ocean.

One notable feature of the Pearl River plume is its pronounced seasonality due to monsoons and freshwater discharge, which affect both the absolute amount of nutrient loading and the spatial distribution of nutrients (Yin et al. 2000, Yin 2002). In summer, the southwest monsoon dominates, and the Pearl River plume flows to the east and mixes with South China Sea oceanic water in south Hong Kong coastal waters (Yin 2002, Dong et al. 2004, Yin et al. 2004). In winter, the northeast monsoon prevails, causing the Pearl River plume to flow to the western side of the estuary and exert little influence on Hong Kong coastal waters. Pearl River discharge also displays a strong seasonality, with high freshwater discharge from April to September (the wet season) and low discharge between October and March (the dry season) (Yin et al. 2000, Dong et al. 2004).

This study aims to determine how variability of nutrient loading in Hong Kong coastal waters affects phytoplankton and microzooplankton biomass, phytoplankton growth rate and grazing mortality by microzooplankton. We chose 2 contrasting stations for a comparative investigation of annual cycles. One western estuarine station (WE, original number NM3, 17 m depth) is in the Pearl River estuary, and the other eastern oceanic one (EO, original number PM7, 19 m depth) is located in a semi-enclosed bay outside of the river plume's influence, being mostly influenced by the oceanic South China Sea (Fig. 1). Since WE is near the eastern boundary of the river estuary, we expected that it would exhibit high nutrient loading

and nutrient-sufficient phytoplankton growth for much of the year, particularly during the spring–summer wet season, due to both the high freshwater discharge and the river plume direction at this time. In contrast, nutrient-limited growth was anticipated at EO for much of the year. Growth and grazing rates were estimated using the seawater dilution technique (Landry & Hassett 1982, as modified by Landry et al. 1995), and community structure was assessed using microscopy and flow cytometry.

MATERIALS AND METHODS

Dilution experiments (Landry & Hassett 1982) were conducted monthly at WE (22° 21.32' N, 113° 56.78' E) and EO (22° 20.45' N, 114° 17.70' E) in Hong Kong coastal waters from February 2007 to February 2008 (Fig. 1). Temperature and salinity were measured using a YSI 6600 multi-probe sensor, which was calibrated before each survey. Seawater was collected from the surface by directly immersing 20 l polycarbonate (PC) carboys into the sea, and experiments were set up within 2 h after sampling. Dilution treatments were made by diluting measured amounts of unfiltered seawater with particle-free water. Particle-free water was prepared by filtering seawater through a 0.2 µm filter capsule (Pall) by gravity into a clean 10 l carboy. The unfiltered seawater was gently screened
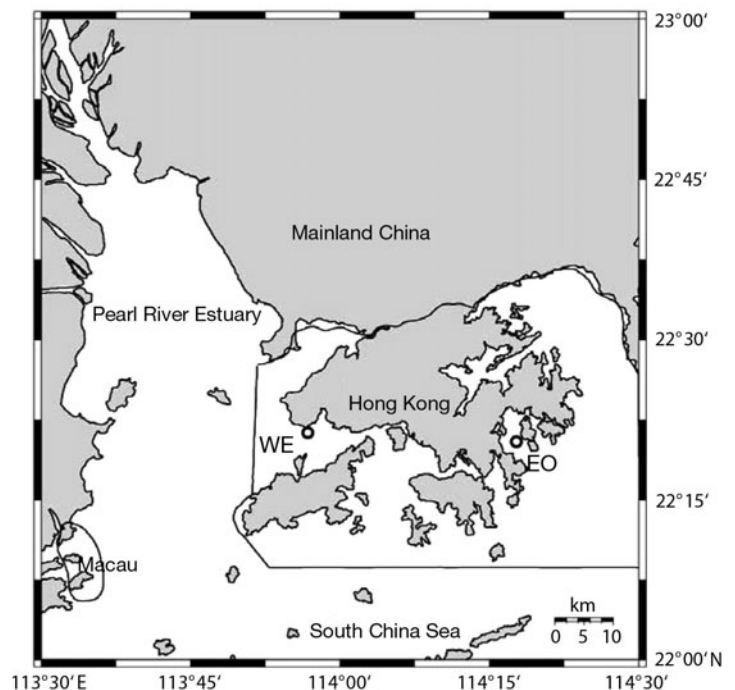

Fig. 1. Sampling stations in the Pearl River estuary (WE) and Hong Kong coastal waters (EO)

through a 200 µm mesh to exclude mesozooplankton, taking care to minimize damage to microzooplankton during mixing and transfer. Duplicate 2.4 or 1.2 l PC bottles were prepared for 5 dilution treatments with percentages of unfiltered seawater volumes of 7, 25, 50, 73 and 100%. Nitrate (10 µmol l^{-1} final concentration) and phosphate (1 µmol l^{-1} final concentration) were added to promote constant phytoplankton growth. Two bottles filled with unfiltered seawater without nutrient amendment were used as no nutrient controls, and an additional 2 or 3 bottles filled with unfiltered seawater were used for initial sampling. All of the experimental bottles were filled to capacity and incubated in a bath cooled by running seawater for 24 h. The bottles were exposed to natural sunlight without any screening since the water samples were taken from the surface. All filters, tubings, meshes and bottles were acid washed and thoroughly rinsed with ultrapure water before each use.

Chlorophyll *a* (chl *a*) concentrations and picophytoplankton abundances were determined at initial (triplicate) and 24 h (duplicate from each bottle) time points. For initial chl *a* sampling, aliquots of 100 to 500 ml were sequentially filtered through 20 and 2 µm PC membrane filters and GF/F under low vacuum pressure. Size fractionation of chl *a* was not conducted at the 24 h sampling (only GF/F were used). Chlorophylls in the filters were extracted overnight in 90% acetone at 4°C in the dark, and chl *a* was determined using in vitro fluorescence with a Turner Designs Model 7200 fluorometer (Strickland & Parsons 1972). The fluorometer was calibrated against a pure chl *a* standard (Sigma) and checked with a secondary standard each day before measurement.

Samples for measurement of inorganic nutrients (nitrate, nitrite, ammonium, phosphate and silicate) were taken in duplicate from initial sampling bottles, filtered through GF/F, and the filtrates frozen at −20°C until analysis. After thawing at room temperature, the concentrations of inorganic nutrients were determined on a Skalar autoanalyzer (San Plus) following JGOFS protocols (Knap et al. 1996).

Picophytoplankton samples were fixed with 0.2% paraformadehyde (final concentration) and stored at 4°C before being analyzed within 1 d on a Coulter Epics XL benchtop flow cytometer equipped with an air-cooled 15 mW 488 nm laser at a flow rate of 72 µl min^{-1}. One µm yellow-green fluorescent beads (Polysciences) were added to each sample as an internal standard. The samples were run for 2 to 5 min depending on particle concentration, with encounter rates never exceeding 1000 events s^{-1}. The data files were stored as listmode files and analyzed with WINMDI 2.8 (developed by J. Trotter). The population of phycoerythrin-containing *Synechococcus* (PE-Syn) was distin-

guished from picophytoeukaryotes (Peuk) based on strong orange fluorescence (Olson et al. 1993). *Prochlorococcus* was not detected at our sampling sites. However, a population of small cells without orange fluorescence, presumably *Synechococcus* containing only phycocyanin (PC-Syn), appeared in the summer at WE. All light scattering and fluorescence signals were normalized to the 1 µm beads.

Samples (100 ml) for enumeration of microplankton (including diatoms, ciliates, and dinoflagellates) were fixed with acidic Lugol's solution (5% final concentration) and stored in amber plastic bottles at room temperature. Subsamples of 10 ml were allowed to settle for 24 h, and the microplankton cells were counted with an Olympus IX51 inverted microscope using the Utermöhl method at 200× magnification. To better estimate the standing stocks of microzooplankton for comparison with microzooplankton grazing rates, individual cell biovolumes of ciliates and dinoflagellates were also calculated using geometric formulae that approximated their cell shapes. Biovolume of ciliates was converted to cell carbon using the conversion factor of 0.19 pg C $µm^{-3}$ (Putt & Stoecker 1989). Biovolume of dinoflagellates was converted to cell carbon using the equation: pg C $cell^{-1}$ = 0.76 × volume $(µm^3)^{0.819}$, according to Mender-Deuer & Lessard (2000). Ciliates and diatoms were usually identified to species level, while dinoflagellates were identified to generic level. At least 50 cells were counted for each sample. The average size (pg C $cell^{-1}$) of ciliates or dinoflagellates was calculated as the total biomass (pg C l^{-1}) in a sample divided by the total abundances $(cells^{-1})$.

Assuming exponential growth, we calculated the net growth rate (k_i) of phytoplankton in each dilution treatment using the formula: $k_i = \ln[P_i/(D_i \times P_0)]$, where P_i is the chl *a* concentration or picophytoplankton abundance in the *i*th treatment bottle at 24 h, D_i is the dilution factor (proportion of unfiltered seawater) of the *i*th treatment, and P_0 is the initial chl *a* concentration or picophytoplankton abundance. Growth (μ_n) and mortality (m) rates of phytoplankton were derived by linear regression of net growth rates on dilution factor. *In situ* phytoplankton instantaneous growth rate (μ_0) equaled m plus net growth rate of phytoplankton in control bottles without nutrient amendment. When saturated grazing was observed as a departure from the assumed linear model (Gallegos 1989), we calculated m based on the following equations assuming a type I functional response (Frost 1972):

$$m = m_1, \mu_0 = m + k_{100\%-N}, \text{ if } P_1 > P_0$$
$$m = \mu_n - k_{100\%}, \mu_0 = \mu_n - k_{100\%} + k_{100\%-N}, \text{ if } P_1 < P_0$$

where m_1 = negative value of the slope of the linear regression curve within the non-saturation range, P_1 =

average phytoplankton biomass/abundance through-
out the 24 h incubation period in the least diluted bot-
tle within the non-saturation range, P_0 = initial phyto-
plankton biomass/abundance, $k_{100\%-N}$ = net rate of
phytoplankton growth in the control bottles without
nutrient amendment, $k_{100\%}$ = net rate of phytoplankton
growth in undiluted bottles (100 % treatments) with
nutrient amendment. We defined the non-saturation
range by testing if the data points of the 73 or 100 %
treatments were significant outliers of the regression
curve constituted by data points in the 3 highly diluted
treatments. In applying these alternate calculations of
m, we considered whether grazing saturation may
have been caused by the growth response of phyto-
plankton to the nutrient amendments, i.e. since the ob-
jective of the dilution experiments was to obtain in-
stantaneous microzooplankton grazing rates under *in
situ* environmental conditions, we first compared the
initial chl *a* concentrations (P_0) with the average chl *a*
concentrations in the least diluted bottle within the
non-saturation range (P_1). If $P_1 > P_0$, this indicated that
under *in situ* conditions, phytoplankton had not
reached the level that saturated grazing, and the graz-
ing rate was just the negative value of the slope of the
regression curve within the non-saturation range.
Conversely, if $P_1 < P_0$, this meant that under *in situ* con-
ditions, grazing saturation had already occurred, and
the grazing rate was calculated assuming that grazing
rates for the undiluted treatments with and without nu-
trient enrichments were identical (Strom et al. 2007). In
3 cases of positive slopes of the linear regression curve
(negative grazing rates, but not significantly different
from 0), we determined m to be 0 and μ_n to be the aver-
age value of the net growth rates of all 5 dilution treat-
ments (Murrell et al. 2002). Pearson correlation (SPSS)
or multiple regressions (Minitab) were conducted to
assess the relationships between 2 or more variables.

RESULTS

Physical and chemical parameters

While sea surface temperatures at the 2 study sites
showed similar trends, ranging from 16°C in February
to 30°C in July (Fig. 2A), surface salinity trends dif-
fered (Fig. 2B). At the western site WE, surface salinity
remained ~35 from February to April, but significantly
decreased to 8 in June before increasing to >32
between October and February. The salinity fluctua-
tions follow freshwater outflow from the Pearl River,
with the extremely low salinity in June being related to
high river discharge at that time. At the eastern site
EO, surface salinity did not change much throughout
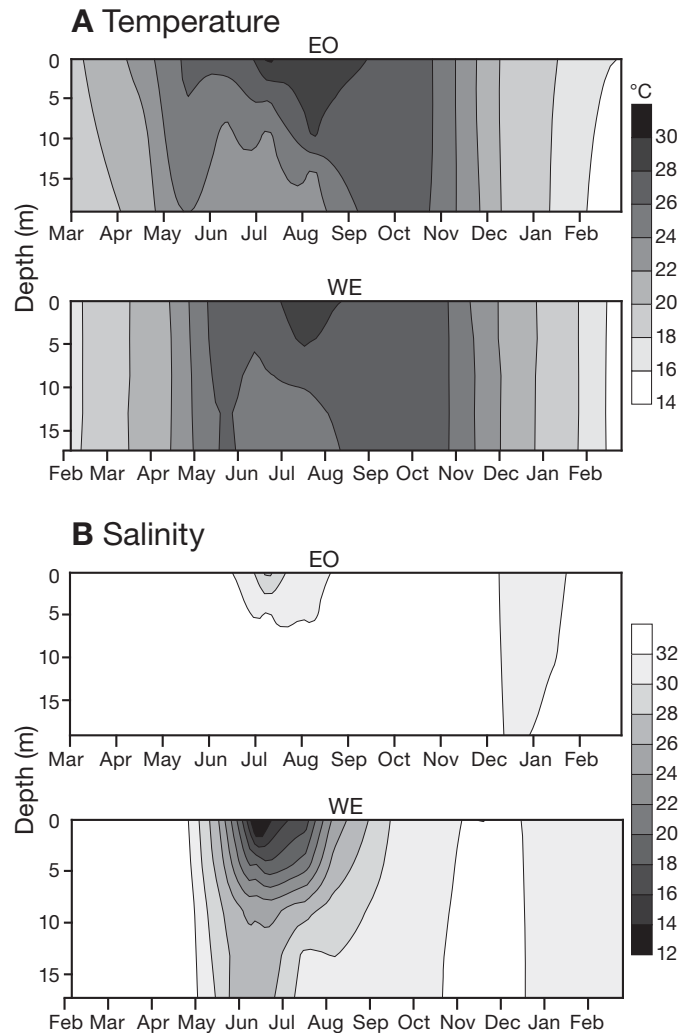the study period, although values were slightly lower

Fig. 2. Seasonal changes in the vertical distribution of
(A) temperature and (B) salinity at Stns EO and WE

during the summer rainy season. The vertical profiles
of temperature and salinity showed that stratification
occurred from May to September. During other
months, the water column was mostly homogeneous.

At EO, surface concentrations of total dissolved inor-
ganic nitrogen (TIN; including nitrate, nitrite and ammo-
nia) ranged from 0.2 to 11 µmol l⁻¹ (mean ± SD = 3.3 ±
3.5 µmol l⁻¹), of which 58 and 36 % were attributable to
nitrate and ammonia, respectively (Fig. 3A). Surface TIN
concentrations were strongly depleted (<0.3 µmol l⁻¹)
during summer months (July, August, and September) at
EO and generally low throughout the spring, except in
June (4.9 µmol l⁻¹) following a heavy rain. The seasonal
peak in surface TIN at EO occurred during winter (No-
vember, December and January). TIN concentrations
were always higher (10-fold) at WE, ranging from 14.9 to
84.1 µmol l⁻¹ (mean ± SD = 33.0 ± 19.4 µmol l⁻¹), of which
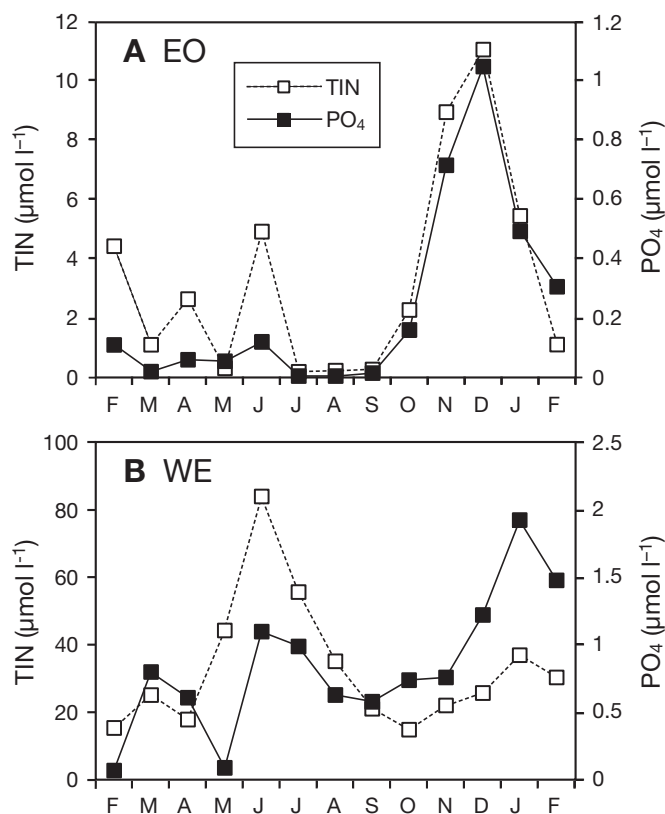54 and 32 % were from nitrate and ammonia, respec-

Fig. 3. Seasonal changes in total inorganic nitrogen (TIN; including nitrate, nitrite and ammonia) and phosphate in surface waters at (A) Stn EO and (B) Stn WE
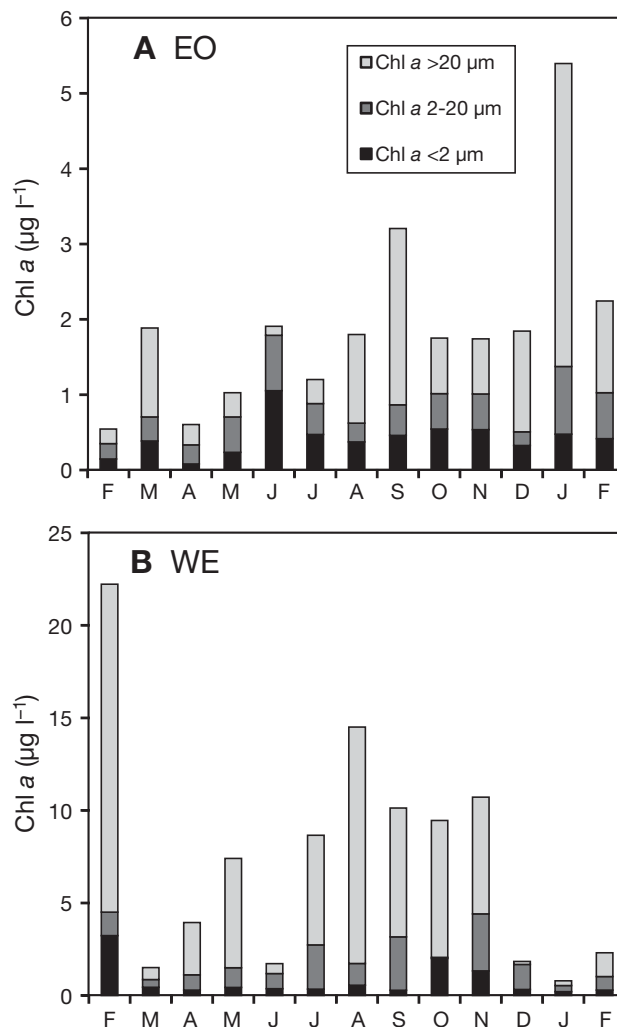

Fig. 4. Seasonal variations in size-fractionated chl a concentrations in surface waters at (A) Stn EO and (B) Stn WE

tively. At this station, surface TIN concentration was negatively correlated with salinity ($r = -0.95$, $p < 0.001$, $n = 13$), with the highest concentration being noted in June when freshwater discharge was most pronounced.

The difference in phosphate concentrations in surface waters at the 2 sampling sites (3.5-fold difference) was not as large as that of TIN. Phosphate ranged from being below the detection limit (0.1 µmol l^{-1}) to 1.1 µmol l^{-1} (mean ± SD = 0.2 ± 0.3 µmol l^{-1}) at EO and from 0.1 to 1.9 µmol l^{-1} (mean ± SD = 0.9 ± 0.5 µmol l^{-1}) at WE (Fig. 3B). Concentrations of TIN and phosphate were positively correlated ($r = 0.90$, $p < 0.001$, $n = 13$) at EO, but not at WE ($r = 0.26$, $p > 0.05$, $n = 13$). Consequently, the N:P ratio of surface water was much higher at WE (data not shown).

Chl a and plankton community structure

Surface chl a concentrations were significantly higher (independent t-test, $p < 0.05$, $n = 13$) at WE (7.3 ± 6.3 µg l^{-1}, range = 0.8 to 22.2 µg l^{-1}) than at EO (1.9 ± 1.3 µg l^{-1}, range = 0.5 to 5.4 µg l^{-1}) (Fig. 4). Based on size-fractionated chl a, microphytoplankton (>20 µm)

dominated phytoplankton biomass at both stations (59 ± 24% at WE; 49 ± 21% at EO), followed by nanophytoplankton (2–20 µm) (27 ± 19% at WE; 27 ± 12% at EO) and picophytoplankton (<2 µm) (14 ± 9% at WE; 25 ± 12% at EO). At both stations, the microphytoplankton size fraction was positively correlated with total chl a ($p < 0.05$) (Fig. 5). At total chl a concentrations >3 to 5 µg l^{-1}, the microphytoplankton size fraction was more or less constant at ~60 to 80% of total chl a. There was no clear seasonality of chl a at either site (Fig. 4). At EO, the lowest chl a concentration was observed in February 2007, while the highest was noted in January 2008 (Fig. 4A). At WE, chl a was generally high in the warm season (May to November) except in June (Fig. 4B). The highest chl a in February at WE was probably an atypical data point signified by post-bloom conditions as discussed below.
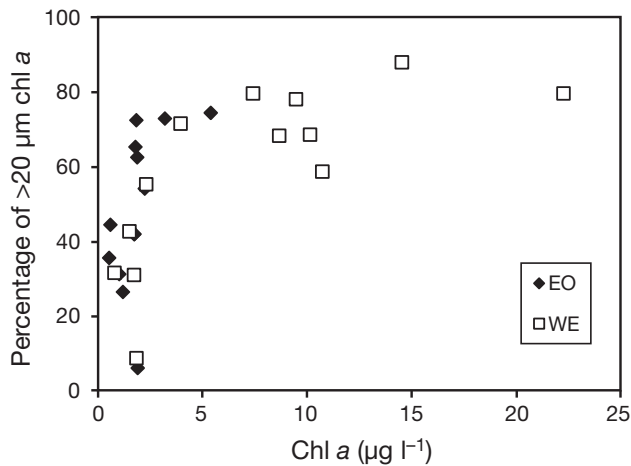
Fig. 5. Percentage of >20 µm chl *a* concentrations versus total chl *a* concentrations in surface waters at Stns EO and WE

Diatoms usually dominated the microphytoplankton size fraction at both stations, with abundances ranging from 10 to 3300 cells ml^{-1} at EO and from 0.4 to 8300 cells ml^{-1} at WE (Table 1). Chain-forming centric diatoms like *Skeletonema* were important at WE, while pennate diatoms like *Pseudo-nitzschia* were occasionally important at EO. At WE, some chlorophytes of

freshwater origin, like *Scenedesmus*, also appeared in June (data not shown), coinciding with high freshwater discharge at this time.

PE-Syn was present during all months at EO, with abundances ranging from 0.3×10^3 to 383×10^3 cells ml^{-1} and a peak in summer (Fig. 6A). Abundance of PE-Syn was positively correlated with temperature (r = 0.78, n = 12, p < 0.01), but not with concentrations of nitrogen or phosphate. Peuk varied from 2×10^3 to 27×10^3 cells ml^{-1} and were generally more abundant in spring (March to June). At WE, PE-Syn was not detected (sample count <10) in February, March, May and June 2007 (Fig. 6B). In other months, PE-Syn abundance was low and highly variable, reaching up to 17×10^3 cells ml^{-1}. Cells enumerated as PC-Syn were only evident at WE from June to September, with densities ranging from 7×10^3 to 150×10^3 cells ml^{-1} and maximum abundance in July. Peuk varied from 2×10^3 to 13×10^3 cells ml^{-1}, with no clear seasonal pattern. The abundances of both PE-Syn and Peuk were significantly higher at EO than at WE (independent *t*-test, p < 0.01).

Both ciliate and dinoflagellate biomasses exhibited large variability with no clear seasonal trends (Fig. 7). Ciliates were dominated by the oligotrichs *Strombidium* and *Strobilidium*, and the mixotroph *Myrionecta rubra* was occasionally important. The average ciliate abundance at WE (14.6 ± 14.3 cells ml^{-1}) was 1.7-fold higher than at EO (8.4 ± 10.8 cells ml^{-1}), while the average ciliate biomass at WE (23.5 ± 28.8 µg C l^{-1}) was 2.6-fold higher than at EO (9.1 ± 12.1 µg C l^{-1}), although the difference was not significant (independent *t*-test, p > 0.05). Similarly, average dinoflagellate abundance at WE (9.7 ± 11.9 cells ml^{-1}) was 1.3-fold higher than at EO (7.4 ± 10.9 cells ml^{-1}) and average dinoflagellate biomass at WE (24.9 ± 30.2 µg C l^{-1}) was 3.4-fold higher than at EO (7.4 ± 6.4 µg C l^{-1}). We assumed that all dinoflagellates, which were mostly dominated by *Protoperidinium*, *Prorocentrum*, *Gyrodinium* and *Gymnodinium*, were functionally phagotrophic (Hlaili et al. 2007). Pooling all the data, ciliate and dinoflagellate biomasses were both positively correlated with chl *a* (r = 0.49 and 0.50 for ciliates and dinoflagellates, respectively; p < 0.05, n = 25). The average sizes of ciliates (1740 ± 1140 pg C cell^{-1}) and dinoflagellates (2260 ± 1360 pg C cell^{-1}) at

Table 1. Dominant diatom species and total diatom abundances (cells ml^{-1}) from February 2007 to January 2008 at Stns EO and WE. The dominant diatom species are ranked according to numerical abundance in each month

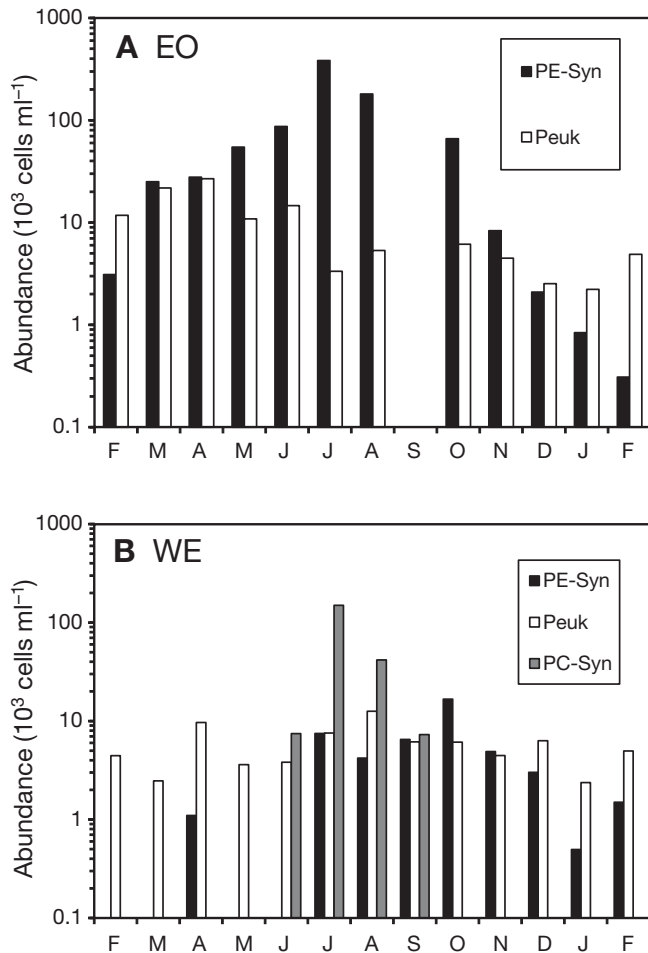|	Month	Dominant diatom species	Total diatom abundance
EO	Feb	*Guinardia striata, Bacillaria paradoxa, G. flaccida*	10
	Mar	*Pseudo-nitzschia delicatissima, Skeletonema costatum*	2580
	Apr	*Cylindrotheca closterium, Skeletonema costatum*	795
	May	*Rhizosolenia fragilissima, Cylindrotheca closterium*	3320
	Jun	*Pseudo-nitzschia delicatissima, Cylindrotheca closterium*	74
	Jul	*Rhizosolenia fragilissima, Leptocylindrus minimus*	490
	Aug	*Pseudo-nitzschia delicatissima, Cylindrotheca closterium*	1350
	Sep	*Bacteriastrum varians, Chaetoceros affinis*	2740
	Oct	*Thalassionema nitzschioides, Skeletonema costatum*	460
	Nov	*Pseudo-nitzschia delicatissima, Skeletonema costatum*	140
	Dec	*Detonula pumila, Chaetoceros curvisetus*	126
	Jan	*Skeletonema tropicum, Thalassiosira rotula*	1040
WE	Feb	*Guinardia delicatula, G. flaccida, Thalassiosira condensata*	680
	Mar	*Cylindrotheca closterium, Skeletonema costatum*	1.7
	Apr	*Skeletonema costatum, Chaetoceros curvisetus*	88
	May	*Skeletonema tropicum, S. costatum*	811
	Jun	*Skeletonema costatum, Pseudo-nitzschia delicatissima*	156
	Jul	*Skeletonema costatum, Guinardia flaccida*	2000
	Aug	*Skeletonema costatum, Pseudo-nitzschia delicatissima, S. tropicum*	1440
	Sep	*Skeletonema costatum, Pseudo-nitzschia delicatissima*	2160
	Oct	*Skeletonema costatum, Chaetoceros curvisetus*	8310
	Nov	*Thalassiosira rotula, Skeletonema costatum*	191
	Dec	*Skeletonema costatum*	2.3
	Jan	*Entomoneis alata, Pleurosigma affine*	0.4

Fig. 6. Seasonal variations in the abundance of picophytoplankton at (A) Stn EO and (B) Stn WE. PE-Syn: phycoerythrin-containing *Synechococcus,* Peuk: picophytoeukaryotes, PC-Syn: phycocyanin-containing *Synechococcus.* Data for September at EO were not available due to technical failure
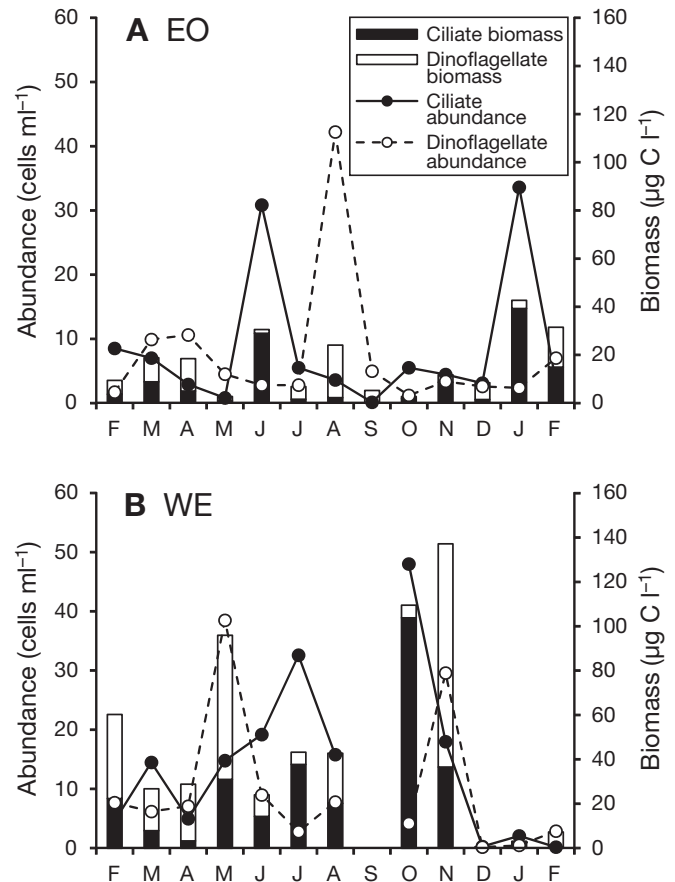

Fig. 7. Seasonal variations in the abundance and carbon biomass of ciliates and dinoflagellates at (A) Stn EO and (B) Stn WE. Data for September at WE were not available due to technical failure

WE were 1.5 and 1.6× larger, respectively, than those at EO (1160 ± 1120 pg C cell^{-1} for ciliates and 1400 ± 630 pg C cell^{-1} for dinoflagellates). The average microzooplankton biomass to chl *a* ratio, which can be used as a relative index of potential top-down control (Corno & Jürgens 2008), was slightly higher at EO (10.2 gC gchl^{-1}) than at WE (7.9 gC gchl^{-1}).

Chl-based rates of phytoplankton growth and microzooplankton grazing mortality

Rates of phytoplankton growth and grazing mortality derived from dilution experiments at the 2 stations are shown in Fig. 8. Growth rates with nutrient amendment (μ_n) ranged from 0.72 to 2.94 d^{-1}, averaging 1.71 ± 0.71 d^{-1} at EO, with a slightly lower range (0.02 to

2.60 d^{-1}) and average (1.31 ± 0.71 d^{-1}) at WE. Highest μ_n estimates were found in late spring (April to May) at EO and steadily declined through summer and fall (Fig. 8). At WE, μ_n showed a unimodal seasonal cycle with a maximum in mid-summer and a minimum in mid-winter (February). Nutrient-amended growth rate (μ_n) was positively correlated with temperature at both stations (r = 0.82 and 0.65, p = 0.001 and 0.02 for WE and EO, respectively, n = 13).

Estimates of growth rate without nutrient amendment (μ_0) varied from 0.12 to 1.92 d^{-1} (mean ± SD = 0.92 ± 0.51 d^{-1}) at EO and from 0.02 to 2.56 d^{-1} (mean ± SD = 1.34 ± 0.73 d^{-1}) at WE. The μ_0 at WE followed the same seasonal pattern as μ_n and showed little evidence of significant nutrient limitation. At EO, however, phytoplankton grew (μ_0) on average at 62% of their maximum (μ_n) potential, and substantial nutrient enhancement of growth rate ($\mu_n \geq 2\mu_0$) was observed throughout the spring and early summer and in January to February 2008 (Fig. 8A). With a mid-summer peak in August, the seasonal pattern for μ_0 at EO was therefore markedly dif-
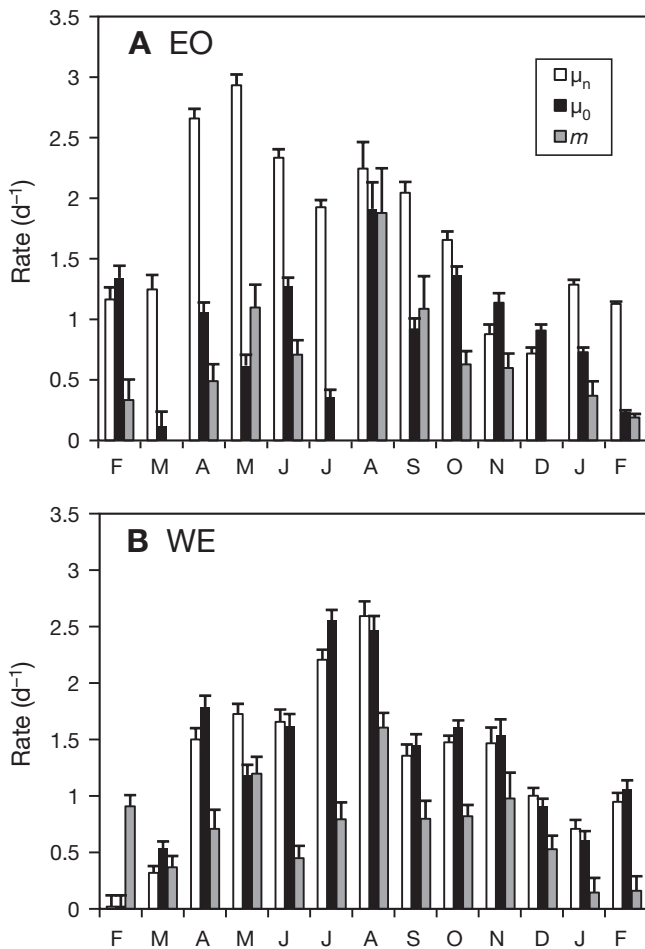
Fig. 8. Seasonal variations in phytoplankton growth rates with nutrient amendment (μ_n), phytoplankton growth rates without nutrient amendment (μ_0), and microzooplankton grazing rates (m) at (A) Stn EO and (B) Stn WE. Error bar = 1 SE
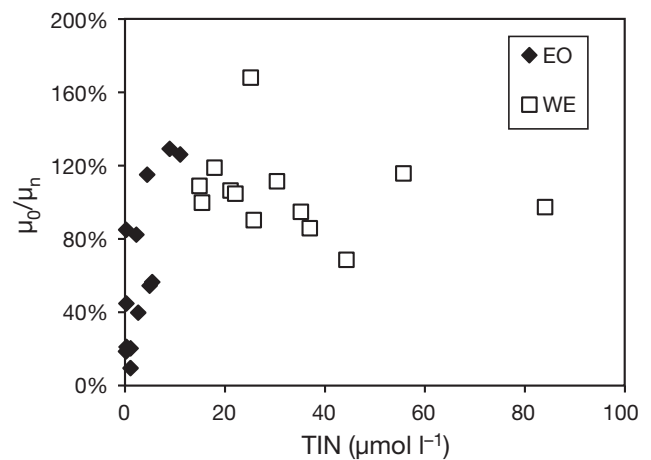

Fig. 9. Phytoplankton nutrient limitation index (μ_0/μ_n) versus total inorganic nitrogen (TIN) concentrations at Stns EO and WE
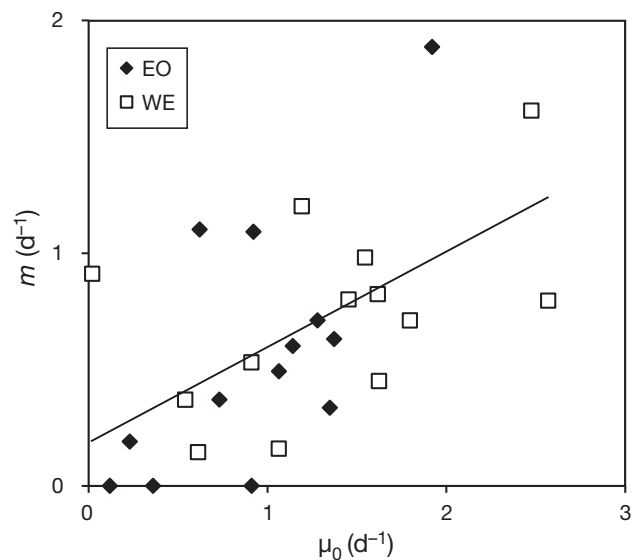

Fig. 10. Microzooplankton grazing rates (m) at different phytoplankton growth rates without nutrient amendment (μ_0) at Stns EO and WE. The solid line represents the least squares fit to all the data points. The Pearson correlation between the 2 variables is significantly positive ($r = 0.56$, $p < 0.01$, $n = 26$)

ferent from that for μ_n. Multiple regressions showed that μ_0/μ_n ratios at EO were significantly positively related to ambient TIN concentrations ($p < 0.05$, $n = 13$) (Fig. 9), but not to phosphate concentrations.

Microzooplankton grazing estimates (m) averaged 0.57 ± 0.54 d^{-1} at EO (range = 0 to 1.88 d^{-1}) and 0.73 ± 0.41 d^{-1} (range = 0.15 to 1.61 d^{-1}) at WE (Fig. 8). At both stations, microzooplankton grazing rates generally increased from March to May and decreased from an August peak through fall and winter. On average, instantaneous rates of phytoplankton growth (μ_0) and microzooplankton grazing (m) were respectively 1.5 and 1.3× higher at WE than at EO. However, μ_0 and m were not significantly different between the 2 stations (paired t-test, $p > 0.05$). m was positively correlated with μ_0 at EO ($r = 0.67$, $p < 0.05$, $n = 13$) and for the pooled dataset ($r = 0.56$, $p < 0.01$, $n = 26$) (Fig. 10), and multiple regressions showed

that this positive correlation was not due to covariation of both rates with temperature at EO. At WE, m was positively correlated with chl a ($r = 0.71$, $p < 0.01$, $n = 13$) and with total microzooplankton (ciliates and dinoflagellates) biomass ($r = 0.58$, $p < 0.05$, $n = 12$) (Fig. 11).

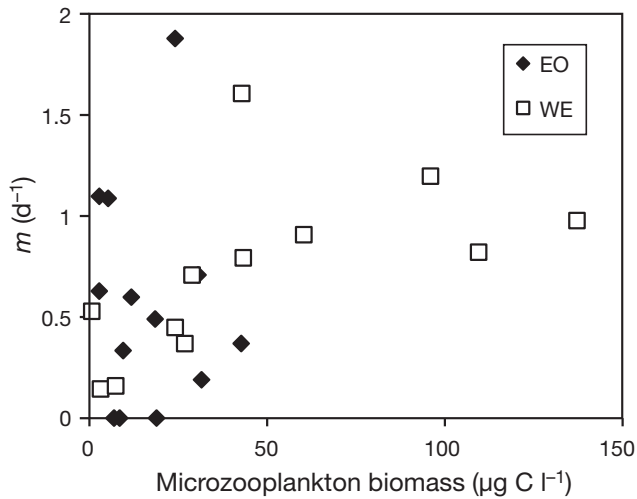Saturated grazing was observed 3× at EO (May and September 2007, January 2008) and 4× at WE (Febru-

Fig. 11. Microzooplankton grazing rates (m) derived from dilution experiments, at different microzooplankton (including both ciliates and dinoflagellates) biomasses

ary, June, August, and September 2007) (Fig. 12). The observed effects in May and September at EO were due to experimental nutrient amendment, since chl a concentrations in control bottles and the ambient environment were below the level where saturated grazing was observed to occur (Fig. 12A,B). Therefore, we assumed that high-food suppression of grazing rates would not have occurred *in situ* during these months.

The percentage of chl a consumed daily by microzooplankton ranged from 0 to 191 % d^{-1} (mean ± SD: 64 ± 54 %, n = 13) at EO and from 18 to 255 % d^{-1} (mean ± SD: 107 ± 70 %, n = 13) at WE. We calculated the mean fraction of primary production consumed by microzooplankton (m/μ_0) after excluding the extreme value of $\mu_0 < 0.2$ (February 2007 at WE) which could give very large m/μ_0. On average, 58 and 50 % of phytoplankton production was grazed by microzooplankton at EO (n = 13) and at WE (n = 12), respectively. Pooling all the data, we found no significant correlation between m/μ_0 and chl a concentration.
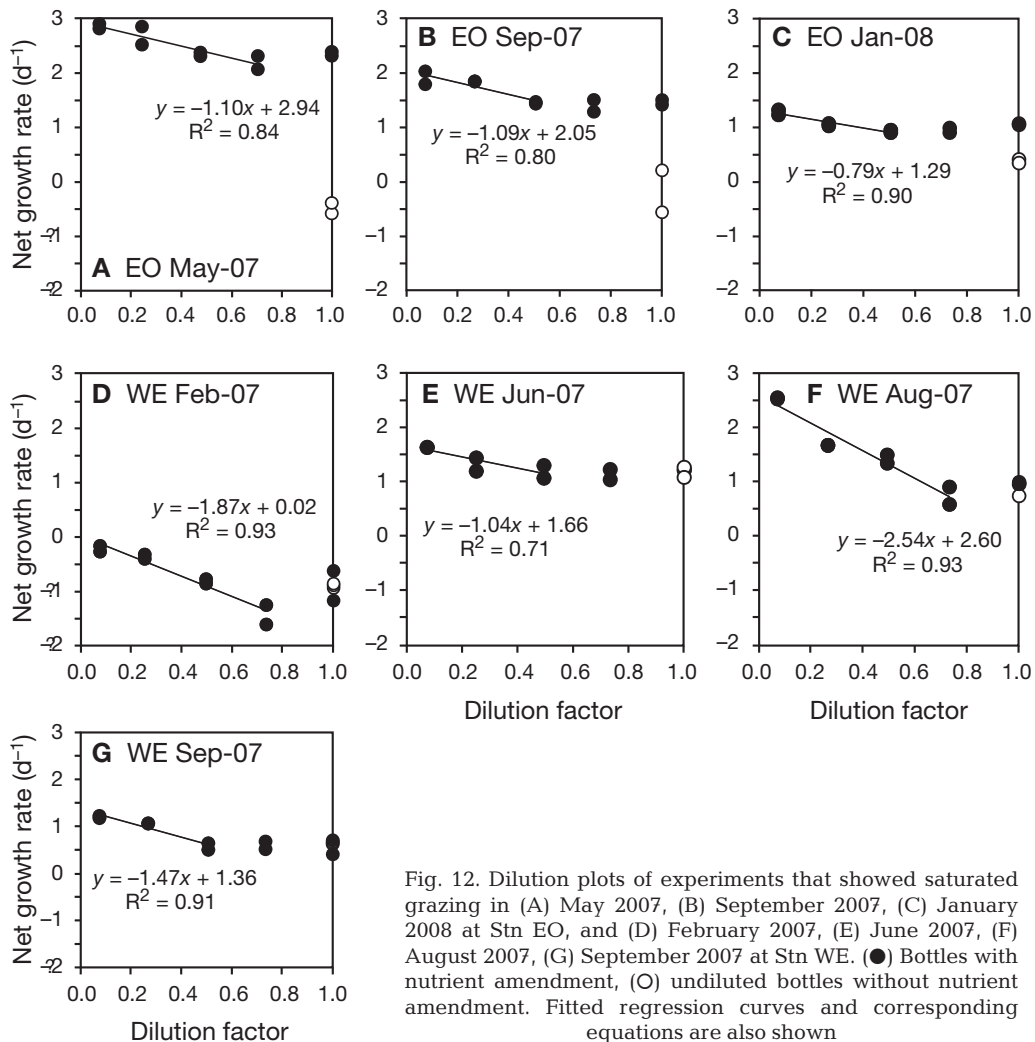

Fig. 12. Dilution plots of experiments that showed saturated grazing in (A) May 2007, (B) September 2007, (C) January 2008 at Stn EO, and (D) February 2007, (E) June 2007, (F) August 2007, (G) September 2007 at Stn WE. (●) Bottles with nutrient amendment, (○) undiluted bottles without nutrient amendment. Fitted regression curves and corresponding equations are also shown

Flow cytometry-based rates of phytoplankton growth and grazing mortality

Monthly estimates of picophytoplankton growth and mortality rates are shown in Fig. 13. Mean growth rates of PE-Syn ($\mu_0 = 1.37 \pm 0.70$ d^{-1}) and Peuk ($\mu_0 = 1.46 \pm 0.86$ d^{-1}) at EO were generally lower than at WE ($\mu_0 = 1.93 \pm 0.84$ d^{-1} and 1.87 ± 1.06 d^{-1}, respectively). However, microzooplankton grazing rates were comparable at both stations, averaging 0.88 ± 0.61 d^{-1} (EO) and 0.84 ± 0.37 d^{-1} (WE) for PE-Syn and 0.92 ± 0.73 d^{-1} (EO) versus 0.86 ± 0.57 d^{-1} (WE) for Peuk. At EO, growth of *Synechococcus* was limited by nutrients ($\mu_0 < \mu_n$) only in May and August, while nutrient limitation of Peuk was apparent only in April and July (data not shown). During the summer period at WE, growth ($\mu_0 = 2.17 \pm 0.53$ d^{-1}) and mortality rates ($m = 1.55 \pm 0.48$ d^{-1}) of PC-S*ynechococcus* were comparable with those of PE-Syn. For both stations, μ_n of PE-Syn was positively correlated with temperature (r = 0.58, p < 0.05 for EO; r = 0.95, p < 0.01 for WE). Significant positive relationships with temperature were also found for μ_n of Peuk at WE (r = 0.72, p < 0.01) and for grazing rates (*m*) on PE-Syn and Peuk at EO (r = 0.62 and 0.68, respectively, p < 0.05). At both stations, μ_0 and *m* for PE-Syn were positively correlated (r = 0.64, p < 0.05 for EO; r = 0.86, p < 0.05 for WE). In addition, μ_0 and *m* of PE-Syn were significantly correlated with those of Peuk at EO (r = 0.88 and 0.78, respectively, p < 0.01). Overall, growth rate estimates for picophytoplankton were significantly higher than for the total chl *a* phytoplankton assemblage (paired *t*-tests, p < 0.01, n = 20 for *Synechococcus,* n = 25 for picophytoeukaryotes). Grazing rates on *Synechococcus* were also marginally significantly higher than those for chl *a* (paired *t*-test, p = 0.05, n = 20).
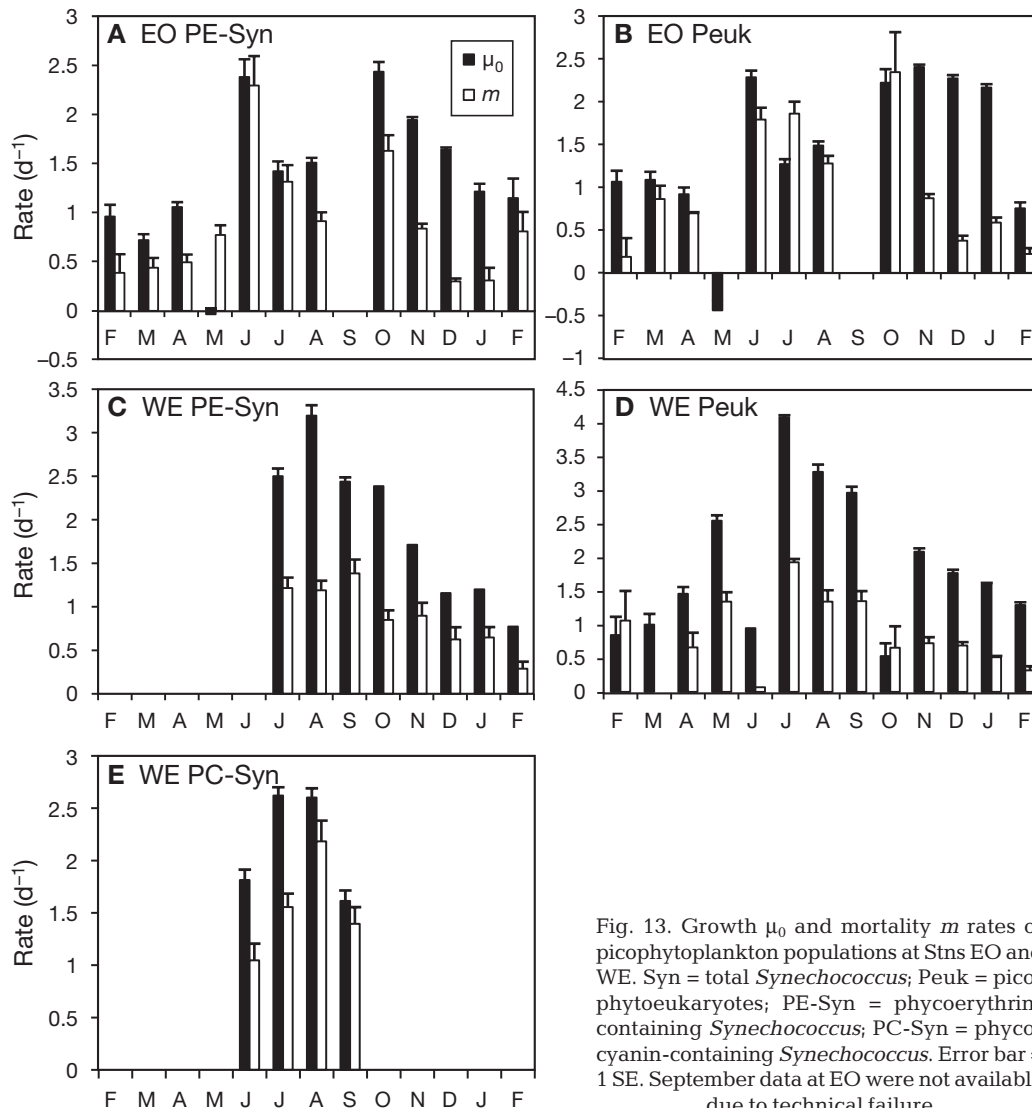

Fig. 13. Growth μ_0 and mortality *m* rates of picophytoplankton populations at Stns EO and WE. Syn = total *Synechococcus*; Peuk = picophytoeukaryotes; PE-Syn = phycoerythrin-containing *Synechococcus*; PC-Syn = phycocyanin-containing *Synechococcus*. Error bar = 1 SE. September data at EO were not available due to technical failure

DISCUSSION

Effects of estuarine nutrient loading on phytoplankton biomass and growth

Nutrient enrichment can increase primary productivity in 2 ways: by increasing phytoplankton biomass and growth rate (O'Brien 1972). Comparing our 2 stations, mean biomass and growth rates were both enhanced at WE, but the magnitude of increase in biomass (3.8×) was substantially greater than that of growth rate (1.5×). Since biomass can vary in proportion to the total inventory of available nutrients while growth rates reach a physiological maximum when nutrients are high, substantially greater biomass than growth rate variability may be a general feature of eutrophic coastal systems (see also synthesis by Calbet & Landry 2004). In an estuarine system similar to our study site, for example, Murrell et al. (2002) observed higher chl a concentrations in the upper Pensacola Bay where nutrients were higher than in the lower bay, but phytoplankton growth and grazing rates were similar at the 2 sites. It appears therefore that the phytoplankton response to estuarine enrichment at WE was more similar to what O'Brien (1972) termed a Type 1 (increase in biomass) rather than Type 2 (increase in growth rate) pattern, which contrasts with recent observations in oligotrophic open oceans (Marañón et al. 2003, Chen et al. 2009).

The insignificance of the difference in phytoplankton growth rates between the 2 stations could be due to their different community compositions and the general allometric relationship between cell size and growth rate (Banse 1982, Chisholm 1992). Diatoms dominated phytoplankton biomass at both stations, but larger diatoms were more abundant at WE due to estuarine eutrophication. The phytoplankton growth rates stimulated by nutrients at WE may thus have been offset by lower maximum growth rates of the larger diatom cells. This effect would also be consistent with the higher average rates of μ_n at EO, which we used as a rough measure of nutrient-saturated maximum growth rates of the phytoplankton assemblage at the 2 stations. Moreover, growth rates of picophytoplankton, which were more abundant at EO, were also higher than those of larger cells (i.e. the community as a whole) in our study.

Although it may seem contradictory to the established view that diatoms usually have the highest growth rates, high growth rates of small phytoplankton, especially in coastal waters, have often been reported in the literature (Raven et al. 2005, Strom et al. 2007). For example, Bec et al. (2008) found that 2 to 3 µm picophytoeukaryotes had the highest growth rates within the ultraphytoplankton range, and their growth rates (up to 3.5 d^{-1}) are comparable with our estimates. Some estimates of *Synechococ-*

cus growth rates (>2 d^{-1}) in this study are also among the highest growth rates of *Synechococcus* recorded in the literature (e.g. Raven et al. 2005). Similar rates of *Synechococcus* growth (up to 2.4 d^{-1}) have also been found in the Mississippi River plume (H. Liu unpubl.). We speculate that some coastal strains of *Synechococcus* are capable of growing at a high rate at the high temperature ($>26°C$) and tropical surface sunlight conditions of our incubations; laboratory studies on the growth rates of isolated *Synechococcus* strains in the study area are underway. However, it is noteworthy that growth rates of picophytoplankton tend to be lower than those of diatoms in the oligotrophic open ocean even in our own studies (Latasa et al. 1997, Brown et al. 1999, Liu et al. 2002, Chen et al. 2009). Changes in phytoplankton composition may thus explain why phytoplankton responses to nutrient injections are more similar to the Type 2 rather than the Type 1 pattern in the open ocean (Marañón et al. 2003, Chen et al. 2009).

Because our incubations were all conducted under surface light conditions, light limitation is not a likely explanation for our lower measured rates of μ_n at WE. Light could, however, be a limiting factor under *in situ* conditions in the 17 m water column when particle load and chl a concentration are high. Occasionally, phytoplankton at WE displayed suboptimal physiological responses, which could not be directly attributed to macro nutrient limitation. For example, in January 2008, photosynthetic photochemical efficiency, F_v/F_m (variable fluorescence/maximum fluorescence yield in the dark; measured by a fluorescence induction and relaxation FIRe system), was only 0.49 compared with a value >0.6 under healthy conditions (B. Chen & H. Liu unpubl. data). Another example was the typical post-bloom condition in February 2007, with high chl a concentration and negligible phytoplankton growth even with nutrient amendment.

Responses of microzooplankton biomass and grazing to eutrophication

Although microphytoplankton dominated phytoplankton biomass at WE, microzooplankton grazing was still the major pathway for phytoplankton loss, accounting for a daily turnover of 101% of chlorophyll and utilization of 50% of the total primary production, which is slightly lower than the global synthesis of Calbet & Landry (2004) for estuarine waters. Parallel experiments on mesozooplankton grazing during the same cruises showed that suspension-feeding metazoans consumed a minor percentage of total primary production, even at WE (M. Chen et al. unpubl.). Heterotrophic dinoflagellates have been shown to feed on chain-forming diatoms (Hansen 1992, Strom &

Strom 1996) and can be important grazers on diatoms (e.g. Landry et al. 2000, 2002, Sherr & Sherr 2007). Therefore, it was not surprising that a large portion of the primary production passes through the microzooplankton before reaching the mesozooplankton, even in coastal waters.

Because our experiments were conducted with surface water under conditions of tropical surface light intensity, it is reasonable to expect that phytoplankton growth rates would decline deeper in the water column where light penetration is sharply reduced. In 2007, the average Secchi disk depth was 3.4 m at EO (range = 2.1 to 5.4 m) and 1.6 m at WE (range = 1.0 to 2.3 m) (data from the Environmental Protection Department, Government of Hong Kong). When stratified, a good portion of the water column could be below the effective euphotic layer of positive phytoplankton growth. If we calculate the extinction coefficient for PAR (photosynthetically available radiation) as roughly 1.4× the Secchi depth (Holmes 1970), then the mean light level in the 19 m water column at EO was 12.8% of incident surface irradiance (I_0), which is ~2× that in the 17 m water column at WE (6.7% of I_0).

Water-column light extinction could affect our interpretation in 2 important ways. First, the fact that 42 to 52% of chl *a* production and roughly comparable fractions of daily picophytoplankton growth escaped grazing by microzooplankton in surface waters does not mean that grazing processes were largely ineffective in regulating phytoplankton over the whole water column. If surplus net production from surface waters was exported to darker depths by sinking or episodic mixing, grazer removal could well have exceeded growth in deep layers, resulting in a substantially lower net water column rate of increase than implied by our surface growth and grazing rate measurements. The seasonally increasing abundance of PE-Syn, especially at EO (Fig. 6), suggests that significant (100×) net accumulation may occur over the course of several months, but the implied growth rates (0.03 d^{-1}) are far lower than the experimental net growth rates of half a doubling or more per day. Given the lack of information on depth relationships, on other local loss processes as well as advective fluxes of water into and out of our research sites, the water-column balances of growth and losses thus cannot be resolved in the present study. However, our estimates of microzooplankton consumption of primary production should be regarded as conservative.

The second way in which potential light limitation could affect the interpretation of our results is in explaining the apparent paradox between picophytoplankton stocks and growth rates at our 2 coastal stations. The measured surface growth rates of *Synechococcus* and picophytoeukaryotes, and the net differences between growth and microzooplankton grazing rates, were all significantly higher at the eutrophic station WE. Their standing stocks, however, were higher at the oceanic site OE. Nevertheless, we cannot reasonably assume that growth rates were higher on average for the water column at WE because the water here was substantially more turbid due to river influence and 3-fold higher mean Chl *a* concentration. We hypothesize that depth-integrated growth rates are likely higher at EO due to deeper light penetration.

Estuarine nutrient enrichment at WE was observed to increase both phytoplankton and microzooplankton biomass by similar extents, which could not have been predicted by classic ecological theory (e.g. Oksanen et al. 1981). Simple nutrient–phytoplankton–zooplankton models, in which zooplankton ingestion and growth rate depend only on phytoplankton biomass, predict that increased nutrient supply rates will increase zooplankton biomass while phytoplankton remain relatively constant (DeAngelis 1992, Sarnelle 1994). Responses of phytoplankton and microzooplankton biomass to nutrient injection in the oligotrophic open ocean may roughly fit this simple model as micrograzers are able to quickly crop down phytoplankton biomass (O'Brien 1972, Marañón et al. 2003, Chen et al. 2009). In open-ocean iron fertilization experiments, however, this has not been the case (e.g. Landry et al. 2000). Our results are also similar to the responses observed in some freshwater experiments (Brett & Goldman 1997) when top-down controls did not extend fully from zooplankton to phytoplankton.

We believe that the difference between simple theory and our field data is partly explained by inefficient transfer from microzooplankton biomass to grazing rates. Although microzooplankton grazing rate was higher on average at WE, the enhancement effect (1.3×) was relatively modest and not significantly different between stations. The mean grazing rate difference was also not proportional to the difference in microzooplankton (ciliates + dinoflagellates) biomass, which was 3.2× higher at WE than at EO. One likely explanation for this disproportionality is grazing saturation (Gallegos 1989, Moigis 2006). When prey densities are above levels that saturate the functional responses of grazers, their reduced clearance rates are reflected in a leveling off of net growth rate versus concentration in the dilution plots (Fig. 12). The microzooplankton thus graze a smaller portion of the primary production, and are less efficient in controlling phytoplankton biomass than they are if their feeding were not saturated. At EO, the only incidence of real saturated grazing which was not artificially induced by nutrient amendment occurred in January, when chl *a* was highest. In contrast, none of the 4 saturated grazing observations at WE was due to nutrient amendment or incubation artifacts

(Fig. 12D–G). Grazing saturation was clearly associated with high ambient concentrations of chl *a*, except in June when freshwater prevailed and low microzooplankton biomass was observed.

As an alternative to grazing saturation, the disproportionately low increase in grazing rate with respect to microzooplankton biomass may also be explained by size effects. For instance, biovolume-specific clearance rates of microzooplankton decrease with increasing cell size (Hansen et al. 1997). Since mean sizes of microzooplankton grazers were larger at WE, their clearance rate per unit of biomass would therefore be expected to be lower than at EO. In addition, if the larger phytoplankton cells at WE were inherently less vulnerable to microzooplankton grazers than the smaller phytoplankton at EO, this would also have the effect of making the increase in grazing impact less than proportional to the increase in grazer biomass.

Seasonal variation in phytoplankton growth and microzooplankton grazing

With highest rates in mid to late summer and lowest in winter, seasonality of phytoplankton growth and microzooplankton grazing rates in our study area appears to be principally defined by temperature rather than nutrient availability, which was highest in winter at EO and in late spring and winter at WE. The positive correlations of both μ_n and *m* with temperature in our study could partly explain why measured rates of phytoplankton growth and microzooplankton grazing are often positively correlated (Murrell et al. 2002, Calbet & Landry 2004, McManus et al. 2007).

In general, the microbial food web was more dominant during summer at EO, with higher abundances of small cells and enhanced microzooplankton grazing rates, while the classic food web was more dominant during winter, with a greater biomass contribution from large cells and lower microzooplankton grazing. In winter, lower microzooplankton metabolic rates (ingestion and growth) may reduce grazing impact disproportionately to phytoplankton growth (Fig. 8), consistent with the observation that maximum growth rates of herbivorous protists decrease more sharply than that of phototrophic protists with decreasing temperature (Rose & Caron 2007). We hypothesize that additional pathways of loss such as flushing or sedimentation might be more important for phytoplankton in winter.

SUMMARY

Relative to Hong Kong coastal waters (EO) removed from Pearl River influence, nutrient enrichment in the river estuary (WE) produces a system of increased biomass of phytoplankton and microzooplankton and higher near-surface rates of phytoplankton growth and microzooplankton grazing. The effect of nutrient enrichment is more apparent in terms of phytoplankton biomass than phytoplankton growth rates, which may be a general property of eutrophic coastal ecosystems. Reduced nutrient availability usually limited phytoplankton growth rates at the eastern coastal station, especially during the spring–summer period, while phytoplankton growth was rarely limited by macronutrients at the estuarine station. Microzooplankton grazing appeared to be weakened at the eutrophic station, but still accounted for >50% of the primary production, which is a likely conservative estimate of microzooplankton grazing role if light limitation significantly reduced growth rates relative to grazing in deeper strata of these turbid ecosystems. In future studies, the depth resolution of growth and grazing processes may provide important new insights into habitat differences among coastal sites and the balance of processes that regulate them.

LITERATURE CITED

Banse K (1982) Cell volumes, maximal growth rates of unicellular algae and ciliates, and the role of ciliates in the marine pelagial. Limnol Oceanogr 27:1059–1071

Bec B, Collos Y, Vaquer A, Mouillot D, Souchu P (2008) Growth rate peaks at intermediate cell size in marine photosynthetic picoeukaryotes. Limnol Oceanogr 53:863–867

Brett MT, Goldman CR (1997) Consumer versus resource control in freshwater pelagic food webs. Science 275:384–386

Brown SL, Landry MR, Barber RT, Campbell L, Garrison DL, Gowing MM (1999) Picophytoplankton dynamics and production in the Arabian Sea during the 1995 southwest monsoon. Deep-Sea Res II 46:1745–1768

Calbet A, Landry MR (2004) Phytoplankton growth, microzooplankton grazing, and carbon cycling in marine systems. Limnol Oceanogr 49:51–57

Chen B, Liu H, Landry MR, Dai M, Huang B, Sun J (2009) Close coupling between phytoplankton growth and microzooplankton grazing in the western South China Sea affected by summer upwelling. Limnol Oceanogr (in press)

Chisholm SW (1992) Phytoplankton size. In: Falkowski PG, Woodhead AD (eds) Primary productivity and biogeochemical cycles in the sea. Plenum Press, New York, p 213–237

Corno G, Jürgens K (2008) Structural and functional patterns of bacterial communities in response to protist predation along an experimental productivity gradient. Environ Microbiol 10:2857–2871

DeAngelis (1992) Dynamics of nutrient cycling and food webs. Chapman & Hall, New York

Dong LX, Su JL, Wong LA, Cao ZY, Chen JC (2004) Seasonal variation and dynamics of the Pearl River plume. Cont Shelf Res 24:1761–1777

Frost BW (1972) Effects of size and concentration of food particles on the feeding behavior of the marine planktonic copepod *Calanus pacificus*. Limnol Oceanogr 17:805–815

Gallegos CL (1989) Microzooplankton grazing on phytoplankton in the Rhode River, Maryland: nonlinear feeding kinetics. Mar Ecol Prog Ser 57:23–33

Hansen PJ (1992) Prey size selection, feeding rates and growth dynamics of heterotrophic dinoflagellates with special emphasis on *Gyrodinium spirale*. Mar Biol 114:327–334

Hansen PJ, Bjornsen PK, Hansen BW (1997) Zooplankton grazing and growth: scaling within the 2–2000 μm body size range. Limnol Oceanogr 42:687–704

Harrison PJ, Yin K, Gan J, Liu H, Lee JHW (2008) Physical–biological coupling in the Pearl River estuary. Cont Shelf Res 28:1405–1415

Sakka Hlaili A, Grami B, Mabrouk HH, Gosselin M, Hamel D (2007) Phytoplankton growth and microzooplankton grazing rates in a restricted Mediterranean lagoon (Bizerte Lagoon, Tunisia). Mar Biol 151:767–783

Holmes RW (1970) The Secchi disk in turbid coastal zones. Limnol Oceanogr 15:688–694

Knap A, Michael A, Close A, Ducklow H, Diskson A (eds) (1996) Protocols for the Joint Global Ocean Flux Study (JGOFS) core measurements. JGOFS Report No. 19, Reprint of the IOC Manuals and Guides No. 29, UNESCO 1994, p 170

Landry MR, Hassett RP (1982) Estimating the grazing impact of marine microzooplankton. Mar Biol 67:283–288

Landry MR, Kirshtein J, Constantinou J (1995) A refined dilution technique for measuring the community grazing impact of microzooplankton, with experimental tests in the central equatorial Pacific. Mar Ecol Prog Ser 120: 53–63

Landry MR, Constantinou J, Latasa M, Brown SL, Bidigare RR, Ondrusek ME (2000) Biological response to iron fertilization in the eastern equatorial Pacific (IronEx II). III. Dynamics of phytoplankton growth and microzooplankton grazing. Mar Ecol Prog Ser 201:57–72

Landry MR, Selph KE, Brown SL, Abbott MR and others (2002) Seasonal dynamics of phytoplankton in the Antarctic Polar Front region at 170° W. Deep-Sea Res II 49: 1843–1865

Latasa M, Landry MR, Schlüter L, Bidigare RR (1997) Pigment-specific growth and grazing rates of phytoplankton in the central equatorial Pacific. Limnol Oceanogr 42: 289–298

Liu HB, Suzuki K, Saino T (2002) Phytoplankton growth, and microzooplankton grazing in the subarctic Pacific Ocean and the Bering Sea during summer 1999. Deep-Sea Res I 49:363–375

Marañón E, Behrendfeld MJ, Gonzalez N, Mouriño B, Zubkov MV (2003) High variability of primary production in oligotrophic waters in the Atlantic Ocean: uncoupling from phytoplankton biomass and size structure. Mar Ecol Prog Ser 257:1–11

McManus GB, Costas BA, Dam HG, Lopes RM, Gaeta SA, Susini SM, Rosetta CH (2007) Microzooplankton grazing of phytoplankton in a tropical upwelling region. Hydrobiologia 575:69–81

Mender-Deuer S, Lessard EJ (2000) Carbon to volume relationships for dinoflagellates, diatoms, and other protist plankton. Limnol Oceanogr 45:569–579

Moigis AG (2006) The clearance rate of microzooplankton as the key element for describing estimated non-linear dilution plots demonstrated by a model. Mar Biol 149:743–762

Murrell MC, Stanley RS, Lores EM, DiDonato GT, Flemer DA (2002) Linkage between microzooplankton grazing and phytoplankton growth in a Gulf of Mexico estuary. Estuaries 25:19–29

O'Brien WJ (1972) Limiting factors in phytoplankton algae. Science 178:616–617

Oksanen L, Fretwell SD, Arruda J, Niemela P (1981) Exploitation ecosystems in gradients of primary production. Am Nat 118:240–261

Olson RJ, Zettler ER, DuRand MD (1993) Phytoplankton analysis using flow cytometry. In: Kemp P (ed) Handbook of methods in aquatic microbial ecology. Lewis Publishers, Boca Raton, FL, p 175–186

Putt M, Stoecker D (1989) An experimentally determined carbon:volume ratio for marine 'oligotrichous' ciliates from estuarine and coastal waters. Limnol Oceanogr 34: 1097–1107

Raven JA, Finkel ZV, Irwin AJ (2005) Picophytoplankton: bottom-up and top-down controls on ecology and evolution. Vie Milieu 55:3–4

Rose JM, Caron DA (2007) Does low temperature constrain the growth rates of heterotrophic protists? Evidence and implications for algal blooms in cold waters. Limnol Oceanogr 52:886–895

Sarnelle O (1994) Inferring process from pattern: trophic level abundances and imbedded interactions. Ecology 75: 1835–1841

Sherr EB, Sherr BF (2007) Heterotrophic dinoflagellates: a significant component of microzooplankton biomass and major grazers of diatoms in the sea. Mar Ecol Prog Ser 352:187–197

Strickland JDH, Parsons TR (1972) A practical handbook of seawater analysis, 2nd edn. Bull Fish Res Board 167: 201–203

Strom SL, Strom MW (1996) Microplankton growth, grazing, and community structure in the northern Gulf of Mexico. Mar Ecol Prog Ser 130:229–240

Strom SL, Macri EL, Olson MB (2007) Microzooplankton grazing in the coastal Gulf of Alaska: variations in top-down control of phytoplankton. Limnol Oceanogr 52: 1480–1494

Yin KD (2002) Monsoonal influence on seasonal variations in nutrients and phytoplankton biomass in coastal waters of Hong Kong in the vicinity of the Pearl River estuary. Mar Ecol Prog Ser 245:111–122

Yin KD (2003) Influence of monsoons and oceanographic processes on red tides in Hong Kong waters. Mar Ecol Prog Ser 262:27–41

Yin KD, Qian PY, Chen JC, Hsieh DPH, Harrison PJ (2000) Dynamics of nutrients and phytoplankton biomass in the Pearl River estuary and adjacent waters of Hong Kong during summer: preliminary evidence for phosphorus and silicon limitation. Mar Ecol Prog Ser 194:295–305

Yin KD, Zhang JL, Qian PY, Jian WJ, Huang LM, Chen JF, Wu MCS (2004) Effect of wind events on phytoplankton blooms in the Pearl River estuary during summer. Cont Shelf Res 24:1909–1923